8830 *Biochemistry* **2009,** *48,* 8830–8841
DOI: 10.1021/bi901018q

BIOCHEMISTRY
including biophysical chemistry & molecular biology
Article

Complete Characterization of the Seventeen Step Moenomycin Biosynthetic Pathway[†]

Bohdan Ostash,[‡,∥,#] Emma H. Doud,[‡,§,#] Cecilie Lin,[‡,§] Iryna Ostash,[‡,∥] Deborah L. Perlstein,[‡] Shinichiro Fuse,[§,⊥] Manuel Wolpert,[‡] Daniel Kahne,[§] and Suzanne Walker*[,‡]

[‡]*Department of Microbiology and Molecular Genetics, Harvard Medical School, Boston, Massachusetts 02115, and* [§]*Department of Chemistry and Chemical Biology, Harvard University, Cambridge, Massachusetts 02138.* [∥]*Current address: Department of Genetics and Biotechnology, Ivan Franko National University of L'viv, Grushevskogo st. 4, L'viv 79005, Ukraine.* [⊥]*Current address: Department of Applied Chemistry, Graduate School of Science and Engineering, Tokyo Institute of Technology, 2-12-1, Ookayama, Meguro, Tokyo 152-8552, Japan.* [#]*These authors contributed equally to this work.*

Received June 18, 2009; Revised Manuscript Received July 28, 2009

ABSTRACT: The moenomycins are phosphoglycolipid antibiotics produced by *Streptomyces ghanaensis* and related organisms. The phosphoglycolipids are the only known active site inhibitors of the peptidoglycan glycosyltransferases, an important family of enzymes involved in the biosynthesis of the bacterial cell wall. Although these natural products have exceptionally potent antibiotic activity, pharmacokinetic limitations have precluded their clinical use. We previously identified the moenomycin biosynthetic gene cluster in order to facilitate biosynthetic approaches to new derivatives. Here, we report a comprehensive set of genetic and enzymatic experiments that establish functions for the 17 moenomycin biosynthetic genes involved in the synthesis of moenomycin and variants. These studies reveal the order of assembly of the full molecular scaffold and define a subset of seven genes involved in the synthesis of bioactive analogues. This work will enable both in vitro and fermentation-based reconstitution of phosphoglycolipid scaffolds so that chemoenzymatic approaches to novel analogues can be explored.

Peptidoglycan glycosyltransferases (PGTs[1]) are a family of enzymes that assemble the glycan chains of the bacterial cell wall from disaccharide precursors (*1*, *2*). They are potentially important antibacterial targets because their functions are essential, their structures are highly conserved, they have no eukaryotic counterparts, and peptidoglycan biosynthesis is a well-validated pathway for antibiotics (*1*, *3*, *4*). Although there are not yet any clinically used antibiotics that target these enzymes, a family of natural products called the phosphoglycolipids inhibit the PGTs and have potent antibacterial activity against Gram-positive pathogens, including methicillin-resistant *Staphylococcus aureus* and both vancomycin-sensitive and vancomycin-resistant pathogens (*1*, *2*, *5*).

Moenomycin A (**1**) (MmA, Figure 1a) is the prototypical member of the phosphoglycolipid family of antibiotics. It has been widely used as an animal growth promoter but was never developed for human use because it has poor physicochemical properties, including a very long half-life that is presumed to be related to the long lipid chain on the molecule (*6*). It may be possible to develop phosphoglycolipid analogues that have better properties than MmA by altering particular structural features. Recently reported structures of cocomplexes of PGTs bound to moenomycin and to neryl-moenomycin provide information on the mode of binding and on critical protein−ligand contacts, which should facilitate efforts to design analogues (*7*−*12*). The challenge now is to develop approaches to make a wide range of analogues efficiently so that the potential of the phosphoglycolipid antibiotics can be explored (*1*, *2*, *5*).

Efforts to synthesize MmA analogues go back many years, and the total synthesis of MmA was reported in 2006 (*1*, *2*, *5*, *6*, *13*). Thus, fully synthetic approaches to make analogues are available. However, the total chemical synthesis of MmA analogues remains an inefficient process because of the structural complexity of the molecule (*6*, *13*). Biosynthetic or chemoenzymatic approaches provide an alternate, potentially more efficient means, to produce analogues. With this possibility in mind, we recently sequenced the producing organism, *Streptomyces ghanaensis*, in order to identify the genes involved in MmA biosynthesis (*14*). We proposed functions for many of the biosynthetic genes based on sequence analysis, but experimental validation of these functions was not completed. Furthermore, specific functions were not assigned for the five putative glycosyltransferases that make the pentasaccharide, the direction of pentasaccharide assembly was not established, the order of the tailoring modifications was unknown, and the genes involved in the biosynthesis of biologically active scaffolds were not identified. Here, we report a comprehensive set of genetic and enzymatic experiments that illuminate the moenomycin biosynthetic pathway. This work lays the foundation for the development of chemoenzymatic approaches to the synthesis of new PGT inhibitors.

[†]This work was supported by startup funds from Harvard Medical School, NIH grants GM076710 and GM066174, NERCE grant AI057159, a NSF graduate research fellowship for E.H.D., an NIH postdoctoral fellowship for D.L.P., and Broad Institute SPARC Award 2740563 for M.W.

*Corresponding author. Department of Microbiology and Molecular Genetics, Harvard Medical School, 200 Longwood Avenue, Boston, MA 02115. Phone: 617-432-5488. Fax: 617-738-7664. E-mail: suzanne_walker@hms.harvard.edu.

[1]Abbreviations: PGTs, peptidoglycan glycosyltransferases; MmA, moenomycin A; UDP-GlcUA, UDP-glucuronic acid; UDP-GalUA, UDP-galacturonic acid; Ch, chinovosamine; GlcNAc, *N*-acetylglucosamine.

 Published on Web 07/29/2009

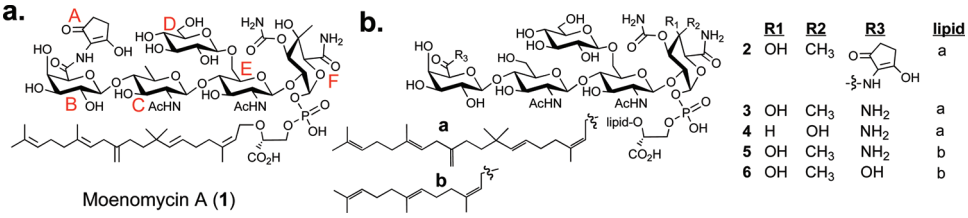

FIGURE 1: Key structures and DNA constructs. (a) Structure of moenomycin A (**1**, MmA). (b) Phosphoglycolipid derivatives of moenomycin: **2** (pholipomycin) produced by strain moeno38-1^{+}pOOB64b^{+}; **3** produced by cosmid moeno38-1; **4** produced by moeno38-1^{+}Δ*moeK5*; **5** and **6** produced by moeno38-1^{+}Δ*moeN5*.

MATERIALS AND METHODS

Antibiotics. Pure MmA was provided by M. Adachi (Dept. of Chemistry and Chemical Biology, Harvard University). The following concentrations of commercially available antibiotics were used for strain selection (μg/mL): ampicillin (100), carbenicillin (100), chloramphenicol (35), kanamycin (50), apramycin (50), hygromycin (100), spectinomycin (200), streptomycin (100), thiostrepton (50), and nalidixic acid (50) (Sigma-Aldrich). UDP-GlcUA was purchased from Sigma-Aldrich. Isoprenoid pyrophosphates were purchased from Isoprenoids, Lc.

Strains and Vector DNAs. *Streptomyces ghanaensis* ATCC14672 and *Bacillus cereus* ATCC19637 were obtained from ATCC. *S. lividans* TK24 was kindly provided by M. Kobayashi (University of Tsukuba, Japan). The methylation-deficient conjugative strain *E. coli* ET12567 (pUB307) (*15*) was obtained from Professor C. P. Smith (Manchester University, U.K.). *E. coli* BW25113 (pIJ790) was obtained from the John Innes Center (Norwich, U.K.). The *S. ghanaensis* strain MO12, which contains a disrupted *moeGT3* gene, and the *S. lividans* strains expressing various subsets of *moe* genes were constructed in this work. The vectors pKC1139, pSET152, pMKI9, and pOOB40 were obtained as described previously (*14*). Plasmid pWQ67 was obtained from Professor C. Whitfield (University of Guelph, Canada) for the expression of epimerase Gla_{KP} (*16*). The integrative vector pSOK804 (*17*) was a gift from S. Zotchev (Norwegian University of Science and Technology, Trondheim, Norway). The expression vector pAF1 (*ori*^{pIJ101} *bla tsr*, P*ermE**, 6His tag) was provided by A. Bechthold (Freiburg University, Germany). Plasmids pKD4 and pCP20 (*18*) were obtained from J. Beckwith (Harvard Medical School, USA). The spectinomycin resistance cassette pHP45 (*19*) was obtained from J.-L. Pernodet (Université Paris-Sud, France). Plasmid pTB146 was obtained from T.G. Bernhardt (Harvard Medical School).

Cloning of moeO5, moeE5, and moeGT1. The *moeO5* gene was initially cloned into the pAF1 vector for expression as a N-terminal His6 fusion in *S. lividans* (pED2; see Supporting Information for complete details of expression and purification). An *E. coli* codon optimized *moeO5* gene (*synO5*) was designed and synthesized by Mr.Gene (see Supporting Information). The gene was delivered in an ampicillin resistant plasmid named pMA_moeO5. *SynO5* was PCR amplified from pMA_moeO5 using primers synO5SUMOf (TTGGTAGAAGAGCAGTTA-ACGCTAGTCCTCAACTG) and synO5SUMOr (CCCGGG-TCAACGGCCAGAACC). These primers introduced the respective restriction enzyme sites SapI and XmaI (underlined). PCR amplification was performed with KOD Hot Start polymerase (Novagen). The PCR product was gel purified, digested with SapI and XmaI, and ligated using T4 DNA ligase (NEB) into the linearized expression plasmid pTB146 to give the N-terminal SUMO/His6-tagged pTBsynO5.

MoeE5 was PCR amplified from cosmid moeno38-1 using primers MoeE5BamHI (AAAAAGGATCCGGTGTCGAG-CGATACACACGG) and MoeE5XhoI (AAAAACTCGAG-CTAC-AGCCGCGGCACGGAC) introducing BamHI and XhoI restriction sites, respectively (underlined). The PCR product was gel purified, digested with BamHI and XhoI, and ligated into linearized vector pET48b using T4 DNA ligase (NEB) to give N-terminal thioredoxin/His6-tagged pET48b-MoeE5.

MoeGT1 was PCR amplified from cosmid moeno38-1 using primers MoeGT1Nde1 (AAACATATGGCTGCCCCCGACC-GAC) and MoeGT1NotI (ATAAAGCGGCCGCTCGGGC-GTC) introducing NdeI and NotI restriction sites (underlined). The PCR product was gel purified, digested with NdeI and NotI, and ligated using T4 DNA ligase (NEB) into linearized vector pET24b to give N-terminal His6-tagged pET24b-MoeGT1.

Expression and Purification of MoeO5, MoeE5, and MoeGT1. The pTBsynO5 expression construct was transformed into BL21(DE3) competent cells (Invitrogen) for protein overproduction. pET48b-MoeE5 and pET24b-MoeGT1 constructs were transformed into Rosetta2(DE3)pLysS (Novagen) competent cells for protein overproduction. Transformants harboring the desired constructs were grown at 37 °C in LB containing 100 μg/mL carbenicillin (for pTBsynO5) or 50 μg/mL kanamycin and 35 μg/mL cloramphenicol (for pET48b-MoeE5 and pET24b-MoeGT1) to an OD_{600} of 0.6. The temperature was reduced to 16 °C, and the cells were induced by the addition of isopropyl-D-thiogalactopyranoside (IPTG) to a final concentration of 1 mM. After an additional 16 h at 16 °C, the cells were harvested by centrifugation (20 min at 5000*g*) and frozen at −80 °C.

pTBsynO5 cells were resuspended in buffer A (50 mM Tris-HCl at pH 7.5, 300 mM NaCl, 5 mM $MgCl_2$, and 3% CHAPS) and incubated at room temperature with rlysozyme, benzonase, and protease inhibitor complexes (Novagen) for 1 h. Cells were then lysed by sonication, and the cell debris was removed by centrifugation (30 min at 14000*g*). The supernatant was diluted with 1.5 volumes buffer B (50 mM Tris-HCl at pH 7.5, 400 mM NaCl, and 5 mM $MgCl_2$) and rocked with TALON resin (Clontech) for 1 h at 4 °C. The resin was collected and washed with buffer B supplemented with 5 mM imidazole by rocking for 30 min at 4 °C, packed into a column, and eluted with 20−200 mM imidazole in buffer B. Fractions containing the target protein (identified by sodium dodecyl sulfate−polyacrylamide gel electrophoresis (SDS−PAGE)) were pooled, desalted, concentrated, flash frozen in liquid nitrogen, and stored at −80 °C. The protein concentration was determined using the Dc Protein Assay (Biorad) using BSA as the standard. The yield of purified MoeO5 was approximately 4 mg/L.

pET48b-MoeE5 and pET24b-MoeGT1 cell pellets were resuspended in buffer C (50 mM Tris-HCl at pH 7.5, 400 mM NaCl, 5 mM $MgCl_2$, and 1% CHAPS) and D (25 mM Tris-HCl

at pH 8, 200 mM NaCl, 5% glycerol, 0.5% CHAPS, and 20 mM imidazole), respectively, supplemented with rlysozyme, benzonase, and protease inhibitor complex (Novagen). After 1 h at room temperature, the cells were lysed by sonication, and the cell debris was removed by centrifugation (30 min at 14000*g*). The supernatant was incubated with Ni-NTA resin (Qiagen) for 30 min at 4 °C. The recovered resin was washed with buffer C or D and packed into a column, and protein was eluted using a stepwise gradient of 5−500 mM imidazole. Fractions containing the target protein (identified by SDS−PAGE) were pooled, desalted, and concentrated. MoeE5 was flash frozen in liquid nitrogen in 20 mM Tris-HCl at pH 7.5, 150 mM NaCl, 10% glycerol and stored at −80 °C. MoeGT1 was stored at 4 °C in 20 mM Tris-HCl at pH 8, 10 mM $MgCl_2$, 10 mM $CaCl_2$, and 10% glycerol. The protein concentration was determined using the Dc Protein Assay (Biorad) using BSA as the standard. The purified yield for MoeE5 was approximately 15 mg/L. The purified yield for MoeGT1 was approximately 4 mg/L.

Characterization of MoeO5. All LC/MS experiments were performed using a Phenomenex Gemini 5u C18 100 Å column (50 mm x 4.6 mm) at a flow rate of 1 mL/min (solvent A: 95:5 water/methanol; solvent B, 60:35:5 isopropanol/methanol/water both with 0.1% ammonium hydroxide as a solvent modifier).

MoeO5 activity assays were performed in 50 mM Tris-HCl at pH 7.5, 300 mM NaCl, 5 mM $MgCl_2$ with 2 mM 3-D-phosphoglyceric acid, and 1 μM MoeO5. Pyrophosphates tested were geranyl, farnesyl, geranylgeranyl, and moenocinyl pyrophosphate (see Supporting Information for the synthesis of moenocinyl pyrophosphate). Reactions were initiated with the addition of 40 μM of isoprenoid pyrophosphate. The reactions were incubated for 1 h at 37 °C and quenched with an equal volume of methanol. The quenched reactions were centrifuged (5 min at 10000*g*) to remove precipitated protein. Reactions were analyzed on an Agilent 1200 LC/MS (conditions described above) with a linear gradient over 10 min. For the farnesyl pyrophosphate reaction, no detectable FPP starting material was observed following a 1 h incubation. Reactions were performed with MoeO5 purified from *S. lividans* (Supporting Information) and with Sumo-MoeO5 purified from *E. coli*, and the results were identical.

For NMR analysis, compound **7** was scaled up and purified by C18 column (Extract-Clean SPE C18 column (Alltech), eluted in methanol) followed by preparative TLC (solvent system: 6:4:0.85 chloroform/methanol/water, run and dried three times). ^{1}H resonances for compound **7** were assigned from one-dimensional (1D) and two-dimensional (2D) COSY spectra based on reported data. Multiplicities are reported by using the following abbreviations: *s* = singlet, *d* = doublet, *t* = triplet, *m* = multiplet, and br = broad. δ_H (500 MHz, D_2O) 1.618 (s, 3H); 1.625 (s, 3H); 1.693 (s, 3H); 1.774 (s, 3H); 2.007−2.035 (m, 2H); 2.094−2.157 (m, 6H); 3.858 (br s, 1H); 3.956−4.038 (m, 3H); 4.126 (br s, 1H); 5.181 (br s, 2H); 5.415 (s, 1H). The stereochemistry of the allylic bond was confirmed to be cis based on 1D NOESYs (see Supporting Information).

Characterization of MoeE5. Reconstitution of MoeE5 activity was performed in reactions containing 20 mM Tris-HCl at pH 7.5 and 1 mM UDP-GlcUA. The reactions were initiated by the addition of 1 μM MoeE5, incubated at 37 °C for 2 h, and quenched by boiling for 5 min followed by centrifugation (5 min at 10000*g*) to remove precipitated protein. Reactions were analyzed by anion-exchange HPLC (Phenomenex Phenosphere SAX 5 μm, 100 Å column, 250 mm × 4.6 mm) on an Agilent 1100 HPLC over a 30 min salt gradient flow rate of 1 mL/min; solvent A = 5 mM $NH_4H_2PO_4$ at pH 4.5; B = 750 mM $NH_4H_2PO_4$ at pH 3.7 (*16*).

Characterization of MoeGT1. Reconstitution of MoeGT1 was carried out in reactions with 50 mM Tris-HCl at pH 7.5, 150 mM NaCl, 5 mM $MgCl_2$, 1 mM UDP-sugar (UDP-GlcUA, UDP-GalUA, or an epimeric mixture of UDP-GlcUA and UDP-GalUA), and 40 μM **7**. Reactions were initiated by the addition of 800 nM MoeGT1, incubated at 37 °C, quenched at specific time points by the addition of 1 volume methanol (see Figure 5 for time points), and centrifuged (5 min at 10000*g*) to remove precipitated protein. Reactions were analyzed on an Agilent 6200 LCMS (conditions described above for MoeO5) with a linear gradient over 10 min. Product and substrate peaks were integrated, normalized, and used to calculate percent conversion in μmols.

Generation of Recombinant S. lividans and S. ghanaensis Strains. Standard molecular biology procedures were used throughout the work (*20*, *21*). For all λ-RED-assisted deletions of *moe* genes within cosmid moeno38-1 (except for *moeGT3*), the entire open reading frame was replaced with a kanamycin resistance cassette (pKD4). The mutated cosmid was introduced into strain DH5α (pCP20) to evict *kanR* as described (*18*). Deletions within the cosmids were confirmed by PCR. To create the Δ*moeGT5*Δ*moeGT3* strain, λ-RED recombination was used to replace *moeGT3* with the disrupted allele *moeGT3::aadA* in the Δ*moeGT5* derivative of moeno38-1 (see Supporting Information). All constructs were transferred into *S. lividans* via intergeneric conjugation. Integration of moeno38-1 and its derivatives into the *S. lividans* genome was confirmed as described (*14*). Gene *moeGT3* was insertionally inactivated in the *S. ghanaensis* genome according to an established procedure (*14*). Plasmid borne copies of the genes were used to complement the gene deletions (see Supporting Information).

Moenomycin Production and Analysis. Small-scale fermentation and purification of moenomycins was performed as described previously (*14*). To obtain pure moenomycin intermediates (>90% as judged by TLC) from recombinant *S. lividans* strains, the following procedure was used. TSB medium (30 mL) in a 250 mL flask containing 70 glass beads (5 mm) was inoculated with 100 μL (approximately 10^4−10^5 cfu) of stock culture (kept in 10.3% sucrose at −20 °C). The flask was incubated on an orbital shaker (240 rpm) for 2 days at 37 °C and then used as a preculture to start the fermentation. Slightly modified R5 medium (*20*) (sucrose: 6% instead of 10.3%; 1 mg/L $CoCl_2$ added after autoclaving) was used as a fermentation medium. Eight 4 L flasks (500 mL of medium per flask) containing beads were grown for 6 days at 37 °C. Using the floor shaker in a warm room fixed at 37 °C provided maximized aeration and optimized antibiotic production compared to smaller incubated shakers at 30 °C. The mycelium was collected by centrifugation and extracted exhaustively with methanol−water (9:1) at 37 °C (when necessary, the pH of extraction mixture was adjusted to 7−7.5 with Tris-HCl). The extract was concentrated, reconstituted in water, and extracted with dichloromethane. The aqueous phase was loaded on a XAD-16 column (30 × 400 mm), washed with water (300 mL), and eluted with methanol (500 mL). Methanol fractions containing the desired compound were combined, concentrated and purified on a Sep-Pak C18 SPE cartridge (Waters) as described. (*22*) Further silica gel flash chromatography or preparative TLC of the extract was performed according to Adachi et al. (*6*) and yielded pure compound

(0.025−0.1 mg/L, depending on the strain). Antibiotic disk diffusion assays, LC-MS, MS/MS, and determination of accurate mass spectra of moenomycins were carried out as described previously (*14*). MIC values (μg/mL) were obtained using a standard microdilution assay. The MIC is defined as the lowest antibiotic concentration that resulted in no visible growth after incubation at 37 °C for 22 h.

^{1}H NMR spectrum of compound **20** was recorded on a Varian Inova 500 (500 MHz) instrument in D_2O (4.80 ppm). Chemical shifts are reported in Supporting Information in parts per million (ppm) units. Primer sequences, strains and plasmids, recombinant DNA construction, generation, verification of *Streptomyces* strains, and structural analysis of MmA intermediates are described in Supporting Information.

RESULTS

Description of the Approach. The MmA biosynthetic genes are located in two clusters on the *S. ghanaensis* chromosome: a three gene operon involved in A ring assembly (*moe* cluster 2) and a larger cluster containing the genes involved in the assembly of the phosphoglycolipid pentasaccharide scaffold (*moe* cluster 1) (*6*, *13*, *14*). We have now reconstituted the biosynthesis of MmA in *S. lividans* using a three-component heterologous expression system. The three components include the previously described integrative cosmid moeno38-1, which contains all but two of the genes of *moe* cluster 1, the replicative plasmid pOOB49f, which supplies the two missing *moe* cluster 1 genes, and the integrative plasmid pOOB64b, which contains the three genes in *moe* cluster 2 (Figure 2) (*14*). To probe the functions of the putative biosynthetic genes, we have constructed a series of derivatives carrying λ-RED-induced single or double gene deletions in cosmid 38-1 or other components of the heterologous expression system (Table 1) and have prepared recombinant *S. lividans* strains expressing the subsets of genes. One gene deletion (*moeGT3*) was prepared in the producing organism, *S. ghanaensis*. We then analyzed the phosphoglycolipids produced by the resulting strains. Because production levels in the heterologous host are low, we made use of exact mass data and previously established fragmentation patterns of the moenomycins to assign structures. MS^2 fragmentation patterns of phosphoglycolipids from fermentation have been extremely well characterized by both Eichhorn et al. and Zehl et al., allowing us to confirm the structures of our compounds (*22*, *23*). One example is shown in Figure 3. Proton NMR spectra were used to confirm assignments in cases where sufficient material was obtained (compounds **7** and **20**). To address polar effects, deletion strains were complemented with plasmid-borne copies of the genes. When genetic approaches could not reveal function (with MoeO5, MoeGT1, and MoeE5), we used biochemical reconstitution of enzymatic activity in vitro to establish substrates and products.

Functions of the Prenyltransferases MoeO5 and MoeN5. Moenomycin contains an irregular isoprenoid chain attached via

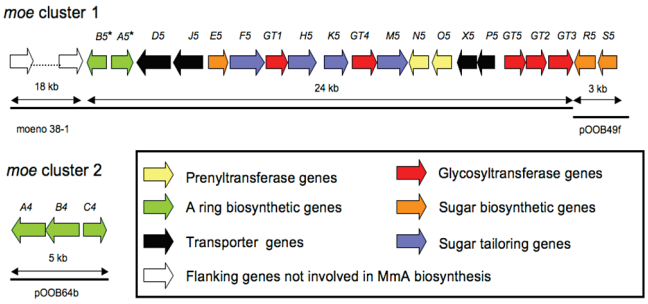

FIGURE 2: Three parental DNA constructs were used to generate all other recombinant cosmids and plasmids described in this study. Cosmid moeno38-1 carries all of *moe* cluster 1 except *moeR5moeS5*. Plasmid pOOB49f carries *moeR5moeS5* under the control of the *ermE* promoter. The three genes in *moe* cluster 2 are carried on plasmid pOOB64b.

Table 1: Data for Phosphoglycolipids from Recombinant Strains and in Vitro Reconstitution

source	compound	retention time (min)	m/z [M − H]$^-$ calculated	m/z [M − H]$^-$ observed
38-1$^+$Δ*moeA5*Δ*B5*	**3**	9.9[b]	1500.6273	1500.6272
38-1$^+$Δ*moeF5*	**8**	3.9[b]	565.2050	565.2055
38-1$^+$Δ*moeGT4*	**9**[a]	4.7[b]	564.2210	564.2221
38-1$^+$Δ*moeGT5*Δ*GT3*	**11**	4.8[b]	781.3160	781.3147
38-1$^+$Δ*moeGT5*	**20**	10.4[b]	1122.4998	1122.5005
38-1$^+$Δ*moeGT2*	**22**	10[b]	1325.5792	1325.5786
38-1$^+$*moeR5*$^+$ Δ*moeH5*	**23**	9.4[b]	1485.6164	1485.6199
38-1$^+$Δ*moeH5*	**24**	9.3[b]	1501.6113	1501.6113
38-1$^+$pBOO64b$^+$ Δ*moeH5*	**24**	9.3[b]	1501.6113	1501.6139
38-1$^+$*moeR5*$^+$ Δ*moeA5*Δ*B5*	**25**	10[b]	1484.6324	1484.6329
38-1$^+$pBOO64b$^+$Δ*moeA5*Δ*B5*	**2**	9.3[b]	1596.6490	1596.6439
38-1$^+$Δ*moeK5*	**4**	9.6[b]	1486.6116	1486.6118
38-1$^+$Δ*moeN5*	**5**	4.1[b]	1365.4861	1365.4867
	6	4.2[b]	1364.5021	1364.5023
S. ghanaensis MO12	**26**[d]	9.2[b]	1418.6007	1418.6016
MoeO5 in vitro	**7**	6.5[c]	389.1729	389.1737
MoeE5 in vitro	**UDP-GalUA**	15.6[d]	579.2793	579.279
	UDP-GlcUA	16.0[d]		
MoeGT1 in vitro	**8**	6.6[c]	565.2050	565.2066

[a]The C4 equatorial epimer of **9** cannot be excluded, but it is not consistent with the reported desmethyl MmA analogue obtained via fermentation nor with evidence that UDP-GalUA is the F ring sugar donor. [b]Column: 250 × 4.6 mm Agilent C_{18} column; conditions are as previously reported (*14*). [c]Column: 100 × 4.6 mm Gemini C_{18} column; conditions are in Supporting Information. [d]The structure (moenomycin C_4) is shown in Supporting Information. HPLC conditions are described in Materials and Methods.

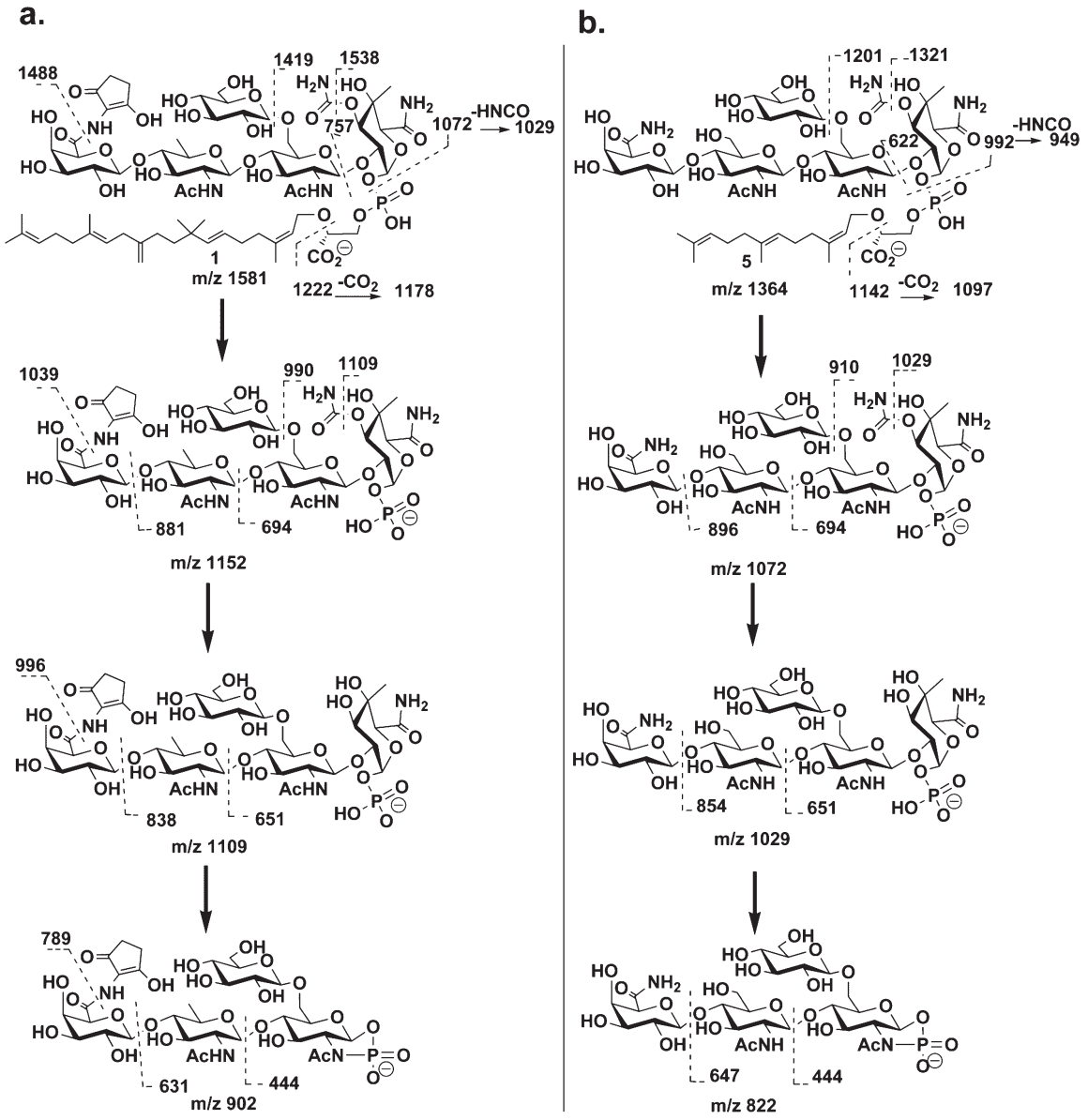

FIGURE 3: Observed fragmentation patterns of (a) moenomycin A (*m*/*z* observed, 1580.6430; calculated, 1580.6535) and (b) compound **5** (*m*/*z* observed, 1364.5023; calcd, 1364.5021), which lacks the C5N unit (A ring), contains farnesyl (C15) rather than moenocinyl (C25) lipid, and has a GlcNAc rather than a chinovosamine C ring for a mass difference of 217. The fragment ions observed for moenomycin A are assigned on the basis of published data by Eichorn et al. (*22*). The corresponding fragment ions are observed for compound **5**. Primary MS^2 data is included in Supporting Information.

a *cis*-allylic ether linkage to phosphoglycerate. On the basis of in silico analysis of moe cluster 1, we previously proposed that *moeO5* and *moeN5*, two putative prenyl transferases, are involved in the assembly of the moenocinyl chain (*14*). MoeO5 is a predicted TIM-barrel protein that shows homology to the prenyl transferases that transfer geranylgeranyl to glycerol phosphate in the first step of archael membrane lipid biosynthesis (*24*, *25*). On the basis of this resemblance, we suggested that MoeO5 forms an ether linkage between D-3-phosphoglyceric acid and an activated moenocinyl chain (*14*). To test this hypothesis, we cloned and expressed MoeO5 in both *S. lividans* and *E. coli* (Supporting Information and Materials and Methods). After purification, MoeO5 was incubated at 37 °C with 2 mM D-3-phosphoglyceric acid and 40 μM of moenocinyl pyrophosphate, synthesized as described in Supporting Information. No product was observed even after an overnight incubation. MoeO5 was then incubated with one of several commercially available prenyl pyrophosphates, including geranyl, farnesyl, and geranylgeranyl pyrophosphate. MoeO5 completely converted farnesyl pyrophosphate to compound **7** within 1 h. The product was purified and shown by NMR to contain a *cis*-allylic ether bond like the natural product (Figure 4, Table 1; see also Supporting Information). It is worth noting that double bond isomerization, although common in prenyl cyclase reactions, has not previously been observed for a prenyl transferase that catalyzes an intermolecular coupling (*26*−*28*). Furthermore, it does not occur in the reactions catalyzed by the archaeal homologues of MoeO5 (*24*, *25*). This and other differences in the substrates and products of the archaeal enzymes compared with MoeO5 suggest that TIM-barrel prenyl transferases, a largely unexplored family of enzymes, may display considerable variability in the types of reactions they catalyze (*29*−*32*).

Since MoeO5 generates a C15 lipid-phosphoglycerate while MmA contains a C25 lipid, we surmised that the other

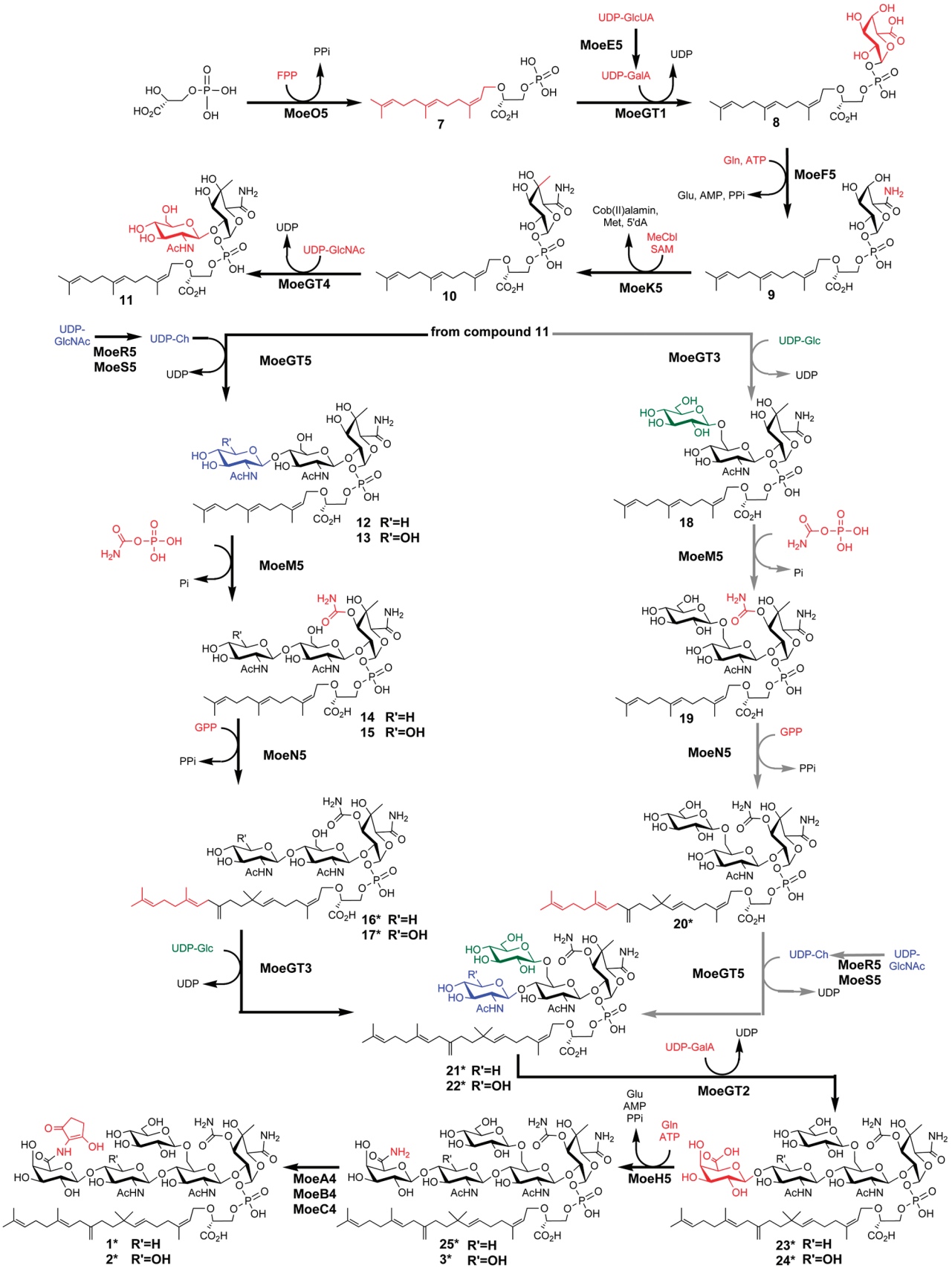

FIGURE 4: Proposed pathway for moenomycin biosynthesis. Solid arrows indicate the order of moenomycin assembly. Structural components shown in red, green, and blue indicate the positions of new moieties in the biosynthetic intermediates. Asterisks (*) indicate biologically active compounds. Structures shown are consistent with exact mass and MS^2 fragmentation data. Stereochemical assignments are consistent with the extensive body of literature on moenomycins isolated from fermentation broths (*49*, *50*). We cannot exclude the possibility that the tailoring enzymes are able to act at multiple points during assembly.

prenyltransferase, MoeN5, must couple the C10 lipid from a pyrophosphate donor to a *z*-farnesylated intermediate in the biosynthetic pathway. Efforts to reconstitute the activity of MoeN5 using starter unit **7** and geranyl pyrophosphate as substrates were unsuccessful (data not shown). However, we found that strain 38-1$^+$Δ*moeN5* accumulates compounds **5** and **6**, which contain farnesyl instead of moenocinyl moieties (Figure 1b and Table 1). Isolation of **5** and **6** from the 38-1$^+$Δ*moeN5* strain confirms that MoeN5 catalyzes C10 prenyl transfer, presumably using geranyl pyrophosphate from primary metabolism as a substrate. A mechanism for the unusual rearrangement that produces the moenocinyl chain was proposed by Arigoni, Welzel, and co-workers (*33*), and this mechanism is consistent with the finding that the C25 chain is constructed via C10 prenyl transfer to a C15-containing intermediate. In cells, MoeN5 apparently only acts on glycosylated intermediates (see below), a finding that may explain our inability to reconstitute its activity using **7** as a substrate.

Functions of the Glycosyltransferases. To probe the functions of each of the five putative glycosyltransferase genes in *moe* cluster 1, we disrupted each of them either singly or in combination (Figure 2). We were able to isolate glycosylated MmA intermediates from strains deficient in MoeGT2, MoeGT3, MoeGT4, and MoeGT5, but not from a strain deficient in MoeGT1. Taken together, these results suggested that MoeGT1 transfers the first sugar to the lipid phosphoglycerate. Based on the structure of the F ring, we speculated that the natural substrate for MoeGT1 is either UDP-glucuronic acid (UDP-GlcUA) or UDP-galacturonic acid (UDP-GalUA). To verify the function of MoeGT1 and assess its donor sugar substrate specificity, we cloned and overexpressed the enzyme as a His-tag fusion in *E. coli*. Following purification, MoeGT1 was incubated with 40 μM of farnesyl phosphoglycerate **7** and 1 mM of either UDP-GlcUA or a mixture of UDP-GlcUA and UDP-GalUA, prepared by incubating UDP-GlcUA with a well-characterized *Klebsiella pneumoniae* UDP-GalUA C4-epimerase from *Klebsiella pneumoniae*, Gla_{KP} (*16*). After 2 h, a product having an exact mass corresponding to compound **8** was detected in both reactions; however, the epimeric mixture of sugars reacted to >80% completion while pure UDP-GlcUA only went to 10% completion (Table 1; see also Supporting Information). Although Michaelis−Menten analysis of MoeGT1 is currently hampered by the low activity of the reconstituted enzyme, a comparison of the two sugar donors following separation of the epimeric mixture showed a clear preference for UDP-GalUA over UDP-GlcUA (0.34 μmol/min for UDP-GalUA and 0.08 μmol/min for UDP-GlcUA, Figure 5). Therefore, UDP-GalUA is assigned as the natural sugar for MoeGT1, consistent with the presence, demonstrated below, of a UDP-GalUA C4 epimerase in *moe* cluster 1.

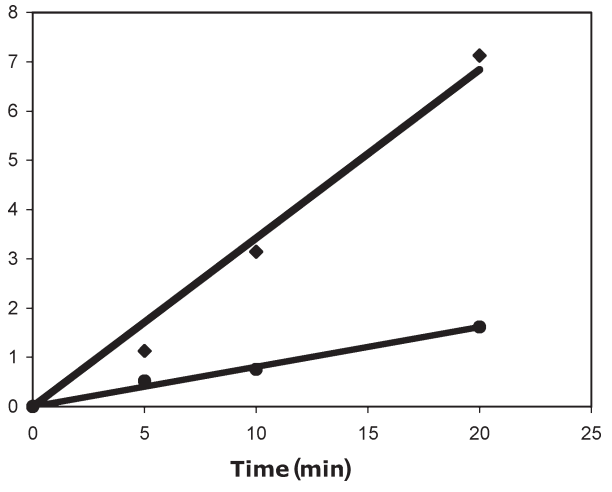

FIGURE 5: Comparison of the MoeGT1 reaction carried out at 37 °C in 50 mM Tris-HCl at pH 7.5, 150 mM NaCl, 5 mM $MgCl_2$, 40 μM compound **7**, 800 nM MoeGT1, and 1 mM of either UDP-GlcUA (●) or UDP-GalUA (♦).

The functions of the other glycosyltransferases were established by analyzing MmA intermediates produced by various gene disruption strains. The recombinant 38-1$^+$Δ*moeGT4* strain was found to accumulate monosaccharide **9** (Figure 4), suggesting that it attaches the E ring sugar. Consistent with this, all strains containing disruptions of *moeGT5*, *moeGT2*, and *moeGT3*, either individually or in combination, were found to produce moenomycin precursors containing the E ring (Figure 4 and Table 1). Furthermore, complementation of the deletion strain with a plasmid borne copy of *moeGT4* produced the desmethylated pentasaccharide **4**. On the basis of these results, we conclude that MoeGT4 acts after MoeGT1 to produce the C15 disaccharide **11**. Upon complementation of the 38-1$^+$Δ*moeGT4* strain, desmethyl compound **4** was produced rather than **3** because the 3′ end of the putative methytransferase *moeK5* gene overlaps with *moeGT4*. Although the *moeGT4* gene deletion affected the expression of *moeK5*, the functional assignments of these genes are not affected (see below; see also Figures 2 and 4).

The order of biosynthesis with respect to the remaining three glycosyltransferases, MoeGT2, MoeGT3, and MoeGT5, indicates a branching pathway. Strains 38-1$^+$Δ*moeGT5* and 38-1$^+$Δ*moeGT2* were found to produce trisaccharide **20** (Figure 4) and tetrasaccharide **22** (Figure 4), respectively. However, the double mutant strain 38-1$^+$Δ*moeGT5*Δ*moeGT3* accumulated C15 disaccharide **11** (Figure 4 and Table 1). Moenomycin analogues lacking the branching glucose (the D ring) are naturally produced in *S. ghanaensis* (*5*). We found that they also accumulate when *moeGT3* is disrupted in the producing organism (*S. ghanaensis* MO12, Table 1). Therefore, we propose that MmA biosynthesis can follow two branches from **11**, depicted in Figure 4, which merge at the stage of the tetrasaccharide **21/22**. In one branch, MoeGT5 attaches the C ring, which can be either chinovosamine (Ch) or *N*-acetylglucosamine (GlcNAc), depending on the presence of *moeR5moeS5* (see below) before MoeGT3 attaches the D ring. In the other branch, MoeGT3 attaches the D ring glucose *before* MoeGT5 attaches the C ring. MoeN5 then extends the lipid chain on trisaccharides **14/15** and **19** to produce **16/17** and **20**. The absence of mono- and disaccharide phosphoglycolipids having the full lipid chain suggests that the moenocinyl chain is assembled in two distinct phases, although the reason for this unusual order of assembly is unclear. Following chain elongation, F ring tailoring (see below), and attachment of the fourth sugar (by either MoeGT5 or MoeGT3 depending on which acted previously), MoeGT2 attaches the B ring sugar to produce the pentasaccharide precursors **23/24** (Figure 4).

Functions of the Sugar Biosynthesis Enzymes. While the gene clusters for most carbohydrate-containing secondary metabolites contain numerous genes involved in the synthesis of nucleotide-sugar building blocks, there are only three genes in the *moe* cluster that appear to be involved in producing NDP-sugar donors. Apparently, the nucleotide-sugar building blocks for moenomycin are siphoned directly from primary metabolism and used largely without further modification. The three sugar biosynthetic genes identified in the *moe* cluster are *moeE5*, which

encodes a putative nucleotide sugar epimerase, and *moeR5-moeS5*, which encode a 4,6-dehydratase/keto-reductase pair. To evaluate the function of these three putative NDP-sugar biosynthetic genes, we constructed the appropriate recombinant strains.

The 38-1$^+$ strain, which is lacking *moeR5moeS5*, accumulates MmA derivative **3** containing GlcNAc in place of chinovosamine (C ring, Figure 1), implying that the missing genes control the conversion of UDP-GlcNAc to UDP-chinovosamine (UDP-Ch, Figure 4). Consistent with this, we found that supplying the missing genes on a plasmid produces a strain, 38-1$^+$*moeR5*$^+$-*moeS5*$^+$, which accumulates a compound (**25**) (Figure 4 and Table 1) containing a methyl at C6 of the C ring. Further studies showed that a 38-1$^+$*moeS5*$^+$ strain yielded only the hydroxymethyl variant **3** (data not shown) (*14*); however, a 38-1$^+$*moeR5*$^+$ strain produced **25** in addition to **3**. It is possible that a homologue of moeS5 in the *S. lividans* genome complements the loss of *moeS5* function in the 38-1$^+$*moeR5*$^+$ strain. Alternatively, MoeR5 may contain both ketoreductase and dehydratase activities. In any event, these results show that moeR5 is required for the biosynthesis of UDP-chinovosamine, the C ring donor for MmA biosynthesis, from UDP-GlcNAc.

To determine the function of the putative nucleotide sugar epimerase *moeE5*, we constructed strain 38-1$^+$Δ*moeE5*, and analyzed its cell extracts. We were unable to detect any phosphoglycolipid compounds in these extracts. Since the apparent glycosyl donor substrate for MoeGT1 is UDP-GalUA (see above), we hypothesized that MoeE5 is responsible for epimerizing UDP-GlcUA obtained from primary metabolism to UDP-GalUA. To test this, we cloned and expressed MoeE5 as a His-tagged fusion in *E. coli*. MoeE5 was incubated with UDP-GlcUA, and the nucleotide-sugar products were then analyzed by anion-exchange HPLC. Pure UDP-GlcUA and the epimeric mixture produced by Gla_{KP}, a well-characterized UDP-GalUA C4-epimerase from *K. pneumoniae*, were used as authentic standards (*16*). MoeE5 was found to convert UDP-GlcUA to a 60:40 mixture of compounds having the same exact mass and identical retention times as those of the authentic standards (Figure 6). Therefore, we conclude that MoeE5 epimerizes UDP-GlcUA to UDP-GalUA to provide the first sugar in MmA biosynthesis.

Functions of the Sugar Tailoring Enzymes. *Moe* cluster 1 contains several genes proposed to encode tailoring enzymes that modify sugars on the growing phosphoglycolipid scaffold. These tailoring enzymes include two genes (*moeA5* and *moeB5*) that are truncated homologues of two of the three genes in *moe* cluster 2 (*moeA4* and *moeB4*, Figure 2). The three genes in *moe* cluster 2 encode a putative aminolevulinate synthase (*moeA4*) as well as two other enzymes proposed to be involved in the assembly and attachment of the A ring. Deletion of *moeA4* from *moe* cluster 2 in the producing organism abolishes A ring formation (*12*). Therefore, the putative aminolevulinate synthase in *moe* cluster 1, *moeA5*, *cannot* complement the loss of *moeA4* and is likely nonfunctional. Expression of moe cluster 2 in the 38-1$^+$Δ*moeA5*Δ*moeB5* deletion strain produces analogues containing the A ring (Supporting Information). These observations indicate that *moe* cluster 2 is required for A ring assembly. Neither *moeA5* nor *moeB5* of moe cluster 1 is required for MmA biosynthesis.

The remaining putative tailoring enzymes in *moe* cluster 1 include *moeF5*, *moeH5*, *moeK5*, and *moeM5*. *MoeF5* and *moeH5* both encode amidotransferases proposed to form primary amides

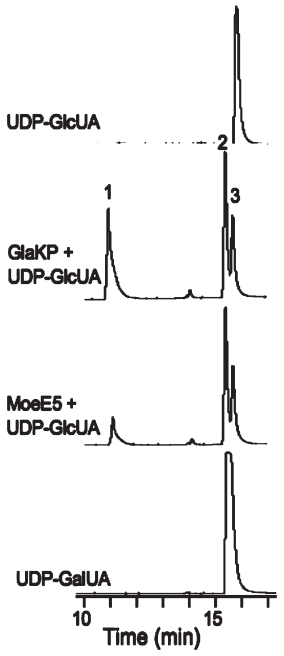

FIGURE 6: Anion-exchange HPLC (see Materials and Methods for conditions) of commercial UDP-GlcUA (peak 3), GlaKP incubated for 2 h at 37 °C with 1 mM UDP-GlcUA in 20 mM Tris-HCl at pH 7.5, MoeE5 incubated for 2 h at 37 °C with 1 mM UDP-GlcUA in 20 mM Tris-HCl at pH 7.5, and UDP-GalUA (peak 2) purified from the MoeE5 reaction. NAD$^+$/NADH (peak 1) is strongly associated with both epimerases, and, although it is likely a necessary coenzyme, it was not necessary to add it exogenously.

from carboxylic acids. However, MmA contains only one unsubstituted amide (on the F ring), which led us to propose previously that moeF5 and moeH5 may work together to catalyze amidotransfer, although we also considered the possibility that only one of the genes was functional. To probe whether both genes are required for MmA biosynthesis, we disrupted each one individually. Strain 38-1$^+$Δ*moeF5* accumulated monosaccharide **8**, which has a carboxyl moiety at C6 instead of a carboxamide group (Figure 4 and Table 1). No methylated monosaccharide precursors or larger phosphoglycolipids could be detected. These results imply that MoeF5 is necessary for F ring carboxamidation and imply that the absence of the carboxamide moiety abolishes unit F methylation and all subsequent transformations.

Strain 38-1$^+$Δ*moeH5* accumulated phosphoglycolipid **24** (Figure 4 and Table 1), indicating that MoeH5 catalyzes carboxamidation of the C6 position of the B ring. This finding may explain the observation that C6 B ring primary amides *and* acids are observed in addition to MmA in fermentations of moenomycins (see Figure 1) (*22*, *23*). Several other secondary metabolites contain C5N units identical to the A ring of MmA, and it has been proposed that these subunits are attached in a process involving attack of an amine on an activated acid to form the corresponding amide (*14*, *34*−*36*). Since an activated acid is a putative precursor in the biosynthesis of MmA, we wondered whether B ring amides are intermediates in the MmA pathway or belong to a different branch of moenomycin metabolism. To determine whether the MoeH5 reaction catalyzes an essential biosynthetic step required for attachment of the unit A chromophore, we coexpressed the genes for unit A biosynthesis (pOOB64b) in strain 38-1$^+$, which produces **3** in the absence of the A ring genes, and also in strain 38-1$^+$Δ*moeH5*, which produces **24** in the absence of the A ring genes (Figure 4). We

observed that pholipomycin **2** (Figure 1b), which contains the A ring, accumulates in the 38-1$^+$pOOB64b$^+$ strain but *not* in the 38-1$^+$Δ*moeH5*pOOB64b$^+$ strain (Table 1) (*5*). The inability of the strain deficient in MoeH5 to make a product containing the A ring implies that carboxylic acid **24** is *not* the direct precursor to **2** (*14*, *37*, *38*). We propose that MoeH5 catalyzes the formation of carboxamides **3/25** as necessary precursors to MmA and pholipomycin, respectively (compounds **1** and **2**, Figure 4). The details of the chemistry involved are not understood, but evidently do not involve attack of an amine on an activated acid. These results may have implications for the biosynthesis of other secondary metabolites containing C5N subunits.

Gene *moeK5* encodes a protein homologous to a recently discovered family of putative radical-SAM, methyl-cobalamin-dependent methyltransferases involved in the biosynthesis of fosfomycin, pactamycin, and a handful of other secondary metabolites (*39*−*45*). We have proposed that MoeK5 controls the methylation of the first sugar (unit F) (*14*). Indeed, strain 38-1$^+$Δ*moeK5* accumulates the desmethylated MmA derivative **4** (Table 1 and Figure 1b). Since previous studies have shown that desmethyl MmA derivatives have the axial stereochemistry at C4 of the F ring (*22*, *46*), as shown in compound **4** (and consistent with our results showing that UDP-GalUA is the F ring precursor), MoeK5-catalyzed methylation must proceed with inversion at the C4 hydroxyl. Because we identified methylated C15-monosaccharide-phosphoglycerate compounds in extracts of several glycosyltransferase deletion strains (Supporting Information), we have concluded that methylation of the F ring sugar occurs at the monosaccharide stage. It must occur following MoeF5-catalyzed carboxamidation of the F ring since only desmethylated compound **8** could be detected in the 38-1$^+$Δ*moeF5* strain (Figure 4 and Table 1).

The remaining tailoring enzyme, MoeM5, was established in our previous study to be a carbamoyltransferase since extracts from a *S. ghanaensis* strain in which the *moeM5* gene was deleted produced only an inactive phosphoglycolipid pentasaccharide lacking the F ring carbamate (see Figure 1a) (*14*). However, the previous study provided no information on when MoeM5 acts in MmA biosynthesis. We analyzed extracts from the set of *moeM5*$^+$ glycosyltransferase deletion strains produced in this study (see Table 1) to try and determine when the carbamate is installed. We detected only descarbamoylated products in extracts accumulating disaccharides; however, only carbamoylated products were detected in extracts accumulating trisaccharides and larger scaffolds. Therefore, we have concluded that carbamoylation occurs primarily at the trisaccharide stage during fermentation (Figure 4). This modification, however, is *not* required to complete the synthesis of the pentasaccharide scaffold since full-length analogues lacking the carbamate are produced in the Δ*moeM5* strain.

On the basis of the preceding studies, we have concluded that *moe* cluster 1 contains 14 demonstrably *functional* biosynthetic genes, while *moe* cluster 2 contains 3. As described below, fewer than half of these 17 biosynthetic genes are required to produce bioactive MmA analogues, an observation that should facilitate efforts to produce novel analogues by pathway engineering.

Antibacterial Activity of Moenomycins Produced in Recombinant Strains. In order to define the subsets of genes required to make bioactive MmA analogues, we assessed the activity of phosphoglycolipids isolated from selected recombinant *S. lividans* strains on a *Bacillus cereus* reporter strain using a disk diffusion assay. Relative compound potencies were assessed by comparing the antibiotic concentrations required to achieve clear zones of inhibition (Figure 7). The results (Figure 7 and Table 2) confirm previous structure−activity relationships reported by Welzel and others but also provide additional insights (*5*, *47*). As expected, monosaccharide compounds **8** and **9** were found to be inactive, while moenocinyl-linked tetra- and pentasaccharides **22** and **3** were found to have activity similar to that of MmA itself. These results confirm the modest role of the A ring in antibiotic activity. The C ring sugar was previously proposed to be an essential part of the minimal pharmacophore, but we have found that DEF trisaccharide **20** also has activity (*5*). In fact, the MIC of **20** against a methicillin sensitive *Staphylococcus aureus* strain was found to be comparable to that of the CEF trisaccharide (8 μg/mL for **20** versus 3 μg/mL for a CEF trisaccharide analogue) (*5*, *6*, *10*, *47*, *48*). The observation that both trisaccharides have biological activity is consistent with structural work showing that the majority of directional contacts between moenomycin and its enzyme target involve *only* the EF-phosphoglycerate portion of the molecule, suggesting that this is the most critical portion of moenomycin for specificity (*10*−*12*). Since both trisaccharides are active, both could serve as starting points for the elaboration of phosphoglycolipid analogues.

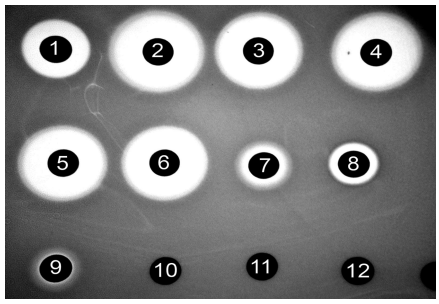

FIGURE 7: Disk diffusion assay of MmA intermediates against reporter strain *B. cereus* ATCC19637. Disks 1 and 2, MmA (**1**), 10 and 100 nmol, respectively; disk 3, compound **22**, 100 nmol; disk 4, compound **25**, 100 nmol; disk 5, compound **23**, 100 nmol; disk 6, compound **4**, 100 nmol; disk 7, mixture of compounds **5** and **6**, 200 nmol; disk 8, compound **20**, 100 nmol; disk 9, mixture of compounds **4** and **5**, 50 nmol; disk 10, extract from 5 g of *S. lividans* TK24 mycelial cake; disk 11 compound **9**, 200 nmol; disk 12, compound **8**, 200 nmol.

Table 2: Relative Antibiotic Activity of MmA Intermediates Based on Disc Diffusion

compound	antibiotic activity[a]
1	+++
2	+++
3	+++
4	+++
5 and **6**	+
7	−
8	−
9	−
11	−
20	++
22	+++
23	+++
24	+++
25	+++

[a] +++ indicates at least 90% as active as MmA, ++ indicates 50−89% activity, + indicates 15−49% activity, and − indicates no visible bioactivity.

Some of the compounds produced in our studies also provide information about the minimum length of the lipid required for biological activity. It was established previously that MmA analogues containing neryl (C10) chains are biologically *inactive* even though they have midnanomolar enzyme inhibitory potencies (*6*). This and other work have indicated an important role for the lipid chain in biological activity (*7*−*11*). It is presumed that the prenyl chain must be long enough to interact with the cell membrane when the pentasaccharide scaffold is bound in the PGT active site so that it can compete with the lipid-anchored substrates, which contain a C55 prenyl chain. We have found that farnesylated compounds **5** and **6**, produced by deleting *moeN5*, show clear zones of inhibition. Therefore, three isoprene units in the prenyl chain are necessary and sufficient to confer biological activity, albeit with a loss in potency. The C25 chain is believed to be responsible for many of the undesirable properties of MmA, including its excessively long half-life and propensity to bind serum. Biologically active analogues containing shorter lipid chains as well as other modifications to improve potency may have more favorable properties than MmA itself, and the studies reported here indicate that it should be possible to reduce the size of the lipid considerably.

DISCUSSION

Summary of the Biosynthetic Pathway and Implications for Analogue Production. The phosphoglycolipids, which target the active site of peptidoglycan glycosyltransferases, remain the only known starting points for the production of potentially useful antibiotics that target these enzymes. In this article, we have described a set of studies that have allowed us to propose a complete biosynthetic pathway for the synthesis of MmA, which should in turn enable the chemoenzymatic production of analogues. The pathway order is reconstructed from deletions of 17 Moe genes and analysis/identification of accumulating intermediates, bolstered by initial enzymatic assays of MoeO5, MoeGT1, and MoeE5. Biosynthesis begins with the coupling of farnesyl pyrophosphate and phosphoglycerate to form starter unit **7**. Sugars are then sequentially attached by a series of glycosyltransferases, starting with the MoeGT1-catalyzed transfer of galacturonic acid (F ring precursor, Figure 4) to **7**. Before additional processing can occur, the galacturonic acid must undergo an obligatory tailoring step by MoeF5, which converts the C6 carboxylic acid to a carboxamide. Methylation at the C4 position, catalyzed by MoeK5, then takes place but is not required for further biosynthetic steps to proceed. MoeGT4 transfers the second sugar, *N*-acetylglucosamine (unit E, GlcNAc), to form the EF disaccharide. MoeGT5 and MoeGT3 then catalyze the addition of the C and D sugar units, respectively (Figure 4), but the order of addition is flexible. At the trisaccharide stage, MoeN5 catalyzes extension of the lipid chain to form the mature C25 isoprenoid chain, and MoeM5 catalyzes carbamoylation of the F ring. Neither modification is required for the other to occur nor for subsequent glycosylations. After tetrasaccharide **21/22** is produced (by either MoeGT3 or MoeGT5), MoeGT2 transfers another galacturonic acid subunit to the scaffold (B ring, Figure 4). The B ring C6 acid is then converted to the corresponding amide by MoeH5; this transformation is required for subsequent attachment of the C5N chromophore by the gene products encoded in *moe* cluster 2.

The results described reveal considerable promiscuity in the moenomycin biosynthetic pathway, which may explain the observation that moenomycins are typically isolated as a complex mixture of related compounds (*23*, *38*). We have found that *except* for unit F carboxamidation, every one of the sugar tailoring reactions can be bypassed without preventing the assembly of the phosphoglycolipid pentasaccharide scaffold. Furthermore, both MoeGT4 and MoeGT5 can accept *either* UDP-GlcNAc or UDP-chinovosamine as donor substrates, explaining the production of pholipomycin (**2**) and moenomycin C_3 as well as moenomycin A (**1**) in both producing organisms and the heterologous expression host (*5*). The complexity of moenomycin mixtures obtained from fermentation has been a major hindrance to efforts to purify intermediates for various uses, including studies directed toward selective chemical derivatization to make novel phosphogycolipid analogues. It should now be possible to simplify the spectrum of moenomycin metabolites produced via fermentation or to optimize the production of new phosphoglycolipid scaffolds for chemoenzymatic synthesis by judicious deletion or overexpression of selected genes in either the producing organism or a suitable heterologous host (*38*).

In addition to establishing gene function and the order of assembly of the pentasaccharide, we have identified the subsets of genes (7 out of the 17 total) required to form biologically active scaffolds. These genes include *moeE5*, *moeO5*, *moeGT1*, *moeF5*, *moeGT4*, *moeM5*, and either *moeGT3* or *moeGT5*. It should be possible to produce phosphoglycolipid scaffolds for further chemical or enzymatic elaboration with 7 or fewer enzymes, depending on the exogenous substrates supplied, making in vitro reconstitution imminently feasible. The ability to reconstitute in vitro the production of small phosphoglycolipid scaffolds will make it possible to explore the substrate tolerances of each enzyme in detail. This information should, in turn, be useful in guiding efforts to engineer heterologous hosts to produce novel phosphoglycolipid antibiotics or precursors for further chemical elaboration.

CONCLUSIONS

We have established functions for the 17 moenomycin biosynthetic genes, determined the order of assembly of the molecule, shown which transformations are required for full assembly of the pentasacharide scaffold, and identified the subsets of 7 genes involved in the production of bioactive analogues. This work will facilitate efforts to make analogues to explore the potential of phosphoglycolipids as useful antibiotics.

ACKNOWLEDGMENT

We thank the following people for the kind donation of strains and plasmids: G. Pettis (pIJ303), M. Bibb (REDIRECT system), J. Beckwith (pKD4, pCP20), J.-L. Pernodet (pHP45), S. Zotchev (pSOK804), C. Whitfield (pWQ67), A. Bechthold (pAF1), and T. Berhnhardt (pTB146). We thank Nicolae Done for the cloning and attempted reconstitution of MoeN5. We thank A. Saghatelian for the use of his Agilent LC/MS QTOF machine in obtaining exact mass data. We thank the NERCE Biomolecule Production Core Laboratory for assistance growing *S. lividans* for protein expression (NIAID U54 AI057159).

SUPPORTING INFORMATION AVAILABLE

Full description of the genetic and enzymatic techniques used in this article. This material is available free of charge via the Internet at http://pubs.acs.org.

REFERENCES

1. Ostash, B., and Walker, S. (2005) Bacterial transglycosylase inhibitors. *Curr. Opin. Chem. Biol. 9*, 459–466.
2. Goldman, R. C., and Gange, D. (2000) Inhibition of transglycosylation involved in bacterial peptidoglycan synthesis. *Curr. Med. Chem. 7*, 801–820.
3. Halliday, J., McKeveney, D., Muldoon, C., Rajaratnam, P., and Meutermans, W. (2006) Targeting the forgotten transglycosylases. *Biochem. Pharmacol. 71*, 957–967.
4. Wright, G. D. (2007) A new target for antibiotic development. *Science 315*, 1373–1374.
5. Welzel, P. (2005) Syntheses around the transglycosylation step in peptidoglycan biosynthesis. *Chem. Rev. 105*, 4610–4660.
6. Adachi, M., Zhang, Y., Leimkuhler, C., Sun, B., LaTour, J. V., and Kahne, D. E. (2006) Degradation and reconstruction of moenomycin A and derivatives: dissecting the function of the isoprenoid chain. *J. Am. Chem. Soc. 128*, 14012–14013.
7. Lovering, A. L., De Castro, L., and Strynadka, N. C. J. (2008) Identification of dynamic structural motifs involved in peptidoglycan glycosyltransfer. *J. Mol. Biol. 383*, 167–177.
8. Lovering, A. L., de Castro, L. H., Lim, D., and Strynadka, N. C. (2007) Structural insight into the transglycosylation step of bacterial cell-wall biosynthesis. *Science 315*, 1402–1405.
9. Yuan, Y., Barrett, D., Zhang, Y., Kahne, D., Sliz, P., and Walker, S. (2007) Crystal structure of a peptidoglycan glycosyltransferase suggests a model for processive glycan chain synthesis. *Proc. Natl. Acad. Sci. U.S.A. 104*, 5348–5353.
10. Yuan, Y., Fuse, S., Ostash, B., Sliz, P., Kahne, D., and Walker, S. (2008) Structural analysis of the contacts anchoring moenomycin to peptidoglycan glycosyltransferases and implications for antibiotic design. *ACS Chem. Biol. 3*, 429–436.
11. Heaslet, H., Shaw, B., Mistry, A., and Miller, A. A. (2009) Characterization of the active site of S. aureus monofunctional glycosyltransferase (Mtg) by site-directed mutation and structural analysis of the protein complexed with moenomycin. *J. Struct. Biol. 167*, 129–135.
12. Sung, M. T., Lai, Y. T., Huang, C. Y., Chou, L. Y., Shih, H. W., Cheng, W. C., Wong, C. H., and Ma, C. (2009) Crystal structure of the membrane-bound bifunctional transglycosylase PBP1b from Escherichia coli. *Proc. Natl. Acad. Sci. U.S.A. 106*, 8824–8829.
13. Taylor, J. G., Li, X., Oberthur, M., Zhu, W., and Kahne, D. E. (2006) The total synthesis of moenomycin A. *J. Am. Chem. Soc. 128*, 15084–15085.
14. Ostash, B., Saghatelian, A., and Walker, S. (2007) A streamlined metabolic pathway for the biosynthesis of moenomycin A. *Chem. Biol. 14*, 257–267.
15. Flett, F., Mersinias, V., and Smith, C. P. (1997) High efficiency intergeneric conjugal transfer of plasmid DNA from *Escherichia coli* to methyl DNA-restricting streptomycetes. *FEMS Microbiol. Lett. 155*, 223–229.
16. Frirdich, E., and Whitfield, C. (2005) Characterization of Gla(KP), a UDP-galacturonic acid C4-epimerase from *Klebsiella pneumoniae* with extended substrate specificity. *J. Bacteriol. 187*, 4104–4115.
17. Sekurova, O. N., Brautaset, T., Sletta, H., Borgos, S. E. F., Jakobsen, O. M., Ellingsen, T. E., Strom, A. R., Valla, S., and Zotchev, S. B. (2004) In vivo analysis of the regulatory genes in the nystatin biosynthetic gene cluster of *Streptomyces noursei* ATCC 11455 reveals their differential control over antibiotic biosynthesis. *J. Bacteriol. 186*, 1345–1354.
18. Datsenko, K. A., and Wanner, B. L. (2000) One-step inactivation of chromosomal genes in *Escherichia coli* K-12 using PCR products. *Proc. Natl. Acad. Sci. U.S.A. 97*, 6640–6645.
19. BlondeletRouault, M. H., Weiser, J., Lebrihi, A., Branny, P., and Pernodet, J. L. (1997) Antibiotic resistance gene cassettes derived from the Omega interposon for use in *E-coli* and *Streptomyces*. *Gene 190*, 315–317.
20. Kieser, T., Bibb, M. J., Buttner, M. J., Chater, K. F., and Hopwood, D. A. (2000) Practical Streptomyces Genetics, The John Innes Foundation, Norwich, U.K.
21. Sambrook, J., and Russel, D. W. (2001) Molecular Cloning: A Laboratory Manual, 3rd ed., Cold Spring Harbor Laboratory Press, Cold Springs Harbor, NY.
22. Eichhorn, P., and Aga, D. S. (2005) Characterization of moenomycin antibiotics from medicated chicken feed by ion-trap mass spectrometry with electrospray ionization. *Rapid Commun. Mass Spectrom. 19*, 2179–2186.
23. Zehl, M., Pittenauer, E., Rizzi, A., and Allmaier, G. (2006) Characterization of moenomycin antibiotic complex by multistage MALDI-IT/RTOF-MS and ESI-IT-MS. *J. Am. Soc. Mass. Spectrom. 17*, 1081–1090.
24. Payandeh, J., Fujihashi, M., Gillon, W., and Pai, E. F. (2006) The crystal structure of (S)-3-O-geranylgeranylglyceryl phosphate synthase reveals an ancient fold for an ancient enzyme. *J. Biol. Chem. 281*, 6070–6078.
25. Zhang, D. L., and Poulter, C. D. (1993) Biosynthesis of archaebacterial ether lipids: Formation of ether linkages by prenyltransferases. *J. Am. Chem. Soc. 115*, 1270–1277.
26. Domingo, V., Arteaga, J. F., del Moral, J. F. Q., and Barrero, A. F. (2009) Unusually cyclized triterpenes: occurrence, biosynthesis and chemical synthesis. *Nat. Prod. Rep. 26*, 115–134.
27. Dewick, P. M. (2002) The biosynthesis of C-5-C-25 terpenoid compounds. *Nat. Prod. Rep. 19*, 181–222.
28. Liang, P. H., Ko, T. P., and Wang, A. H. J. (2002) Structure, mechanism and function of prenyltransferases. *Eur. J. Biochem. 269*, 3339–3354.
29. Anantharaman, V., Aravind, L., and Koonin, E. V. (2003) Emergence of diverse biochemical activities in evolutionarily conserved structural scaffolds of proteins. *Curr. Opin. Chem. Biol. 7*, 12–20.
30. Nagano, N., Orengo, C. A., and Thornton, J. M. (2002) One fold with many functions: The evolutionary relationships between TIM barrel families based on their sequences, structures and functions. *J. Mol. Biol. 321*, 741–765.
31. Caetano-Anolles, G., Yafremava, L. S., Gee, H., Caetano-Anolles, D., Kim, H. S., and Mittenthal, J. E. (2009) The origin and evolution of modern metabolism. *Int. J. Biochem. Cell Biol. 41*, 285–297.
32. Wierenga, R. K. (2001) The TIM-barrel fold: a versatile framework for efficient enzymes. *FEBS Lett. 492*, 193–198.
33. Neundorf, I., Kohler, C., Hennig, L., Findeisen, M., Arigoni, D., and Welzel, P. (2003) Evidence for the combined participation of a C-10 and a C-15 precursor in the biosynthesis of moenocinol, the lipid part of the moenomycin antibiotics. *ChemBioChem 4*, 1201–1205.
34. Hu, Y. D., and Floss, H. G. (2004) Further studies on the biosynthesis of the manumycin-type antibiotic, asukamycin, and the chemical synthesis of protoasukamycin. *J. Am. Chem. Soc. 126*, 3837–3844.
35. Cho, H., Beale, J. M., Graff, C., Mocek, U., Nakagawa, A., Omura, S., and Floss, H. G. (1993) Studies on the biosynthesis of the antibiotic reductiomycin in *Streptomyces xanthochromogenus*. *J. Am. Chem. Soc. 115*, 12296–12304.
36. McAlpine, J. B., Bachmann, B. O., Piraee, M., Tremblay, S., Alarco, A. M., Zazopoulos, E., and Farnet, C. M. (2005) Microbial genomics as a guide to drug discovery and structural elucidation: ECO-02301, a novel antifungal agent, as an example. *J. Nat. Prod. 68*, 493–496.
37. Petricek, M., Petrickova, K., Havlicek, L., and Felsberg, J. (2006) Occurrence of two 5-aminolevulinate biosynthetic pathways in *Streptomyces nodosus* subsp asukaensis is linked with the production of asukamycin. *J. Bacteriol. 188*, 5113–5123.
38. Schuricht, U., Endler, K., Hennig, L., Findeisen, M., and Welzel, P. (2000) Studies on the biosynthesis of the antibiotic moenomycin A. *J. Prakt. Chem. 342*, 761–772.
39. Woodyer, R. D., Li, G. Y., Zhao, H. M., and van der Donk, W. A. (2007) New insight into the mechanism of methyl transfer during the biosynthesis of fosfomycin. *Chem. Commun.* 359–361.
40. Kudo, F., Kasama, Y., Hirayama, T., and Eguchi, T. (2007) Cloning of the pactamycin biosynthetic gene cluster and characterization of a crucial glycosyltransferase prior to a unique cyclopentane ring formation. *J. Antibiot. 60*, 492–503.
41. Unwin, J., Standage, S., Alexander, D., Hosted, T., Horan, A. C., and Wellington, E. M. H. (2004) Gene cluster in *Micromonospora echinospora* ATCC15835 for the biosynthesis of the gentamicin C complex. *J. Antibiot. 57*, 436–445.
42. Nunez, L. E., Mendez, C., Brana, A. F., Blanco, G., and Salas, J. A. (2003) The biosynthetic gene cluster for the beta-lactam carbapenem thienamycin in *Streptomyces cattleya*. *Chem. Biol. 10*, 301–311.
43. Kuzuyama, T., Seki, T., Dairi, T., Hidaka, T., and Seto, H. (1995) Nucleotide-sequence of fortimicin Kl1 methyltransferase gene isolated from *Micromonospora olivasterospora*, and comparison of its deduced amino-acid-sequence with those of methyltransferases involved in the biosynthesis of bialaphos and fosfomycin. *J. Antibiot. 48*, 1191–1193.
44. Hidaka, T., Hidaka, M., Kuzuyama, T., and Seto, H. (1995) Sequence of a P-methyltransferase-encoding gene isolated from a bialaphos-producing *Streptomyces hygroscopius*. *Gene 158*, 149–150.
45. Kuzuyama, T., Hidaka, T., Kamigiri, K., Imai, S., and Seto, H. (1992) Studies on the biosynthesis of fosfomycin. 4. The biosynthetic origin of the methyl-group of fosfomycin. *J. Antibiot. 45*, 1812–1814.

46. El-Abadla, N., Lampilas, M., Hennig, L., Findeisen, M., Welzel, P., Muller, D., Markus, A., and van Heijenoort, J. (1999) Moenomycin A: The role of the methyl group in the moenuronamide unit and a general discussion of structure-activity relationships. *Tetrahedron 55*, 699–722.
47. Welzel, P., Kunisch, F., Kruggel, F., Stein, H., Scherkenbeck, J., Hiltmann, A., Duddeck, H., Muller, D., Maggio, J. E., Fehlhaber, H. W., Seibert, G., Vanheijenoort, Y., and Vanheijenoort, J. (1987) Moenomycin-A: Minimum structural requirements for biological-activity. *Tetrahedron 43*, 585–598.
48. Ritzeler, O., Hennig, L., Findeisen, M., Welzel, P., and Muller, D. (1997) Search for new moenomycin structure-activity relationships. Synthesis of a trisaccharide precursor of a moenomycin analogue. *Tetrahedron 53*, 5357–5357.
49. Hennig, L., Findeisen, M., Welzel, P., and Haessner, R. (1998) H-1 NMR spectroscopic studies of the moenomycins. *Magn. Reson. Chem. 36*, 615–620.
50. Donnerstag, A., Hennig, L., Findeisen, M., Welzel, P., and Haessner, R. (1996) H-1 NMR as a tool for the structure elucidation of moenomycin antibiotics. *Magn. Reson. Chem. 34*, 1031–1035.